PERGAMON

International Journal of Heat and Mass Transfer 43 (2000) 167–177

International Journal of HEAT and MASS TRANSFER

www.elsevier.com/locate/ijhmt

Inlet subcooling effect on heat and mass transfer characteristics in a laminar film flow

Weibo Chen*, Richard N. Christensen

The Ohio State University, Mechanical Engineering, Columbus, OH 43210, USA

Received 8 October 1998; received in revised form 26 April 1999

Abstract

In this paper, a mathematical model for simultaneous heat and mass transfer in an ammonia–water, falling film type of absorber is presented. A nondimensional analysis shows that the overall absorption process can be decomposed into two basic processes: absorption owing to the subcooling of the liquid solution, and absorption owing to the cooling from the wall. Empirical correlations for heat and mass transfer coefficients were developed for film flows with short mixing distances. Numerical results show that both heat and mass coefficients are affected by the subcooling of the inlet solution as well as by the film thickness.

1. Introduction

With the development of absorption technology, more and more attention was drawn to the study of the simultaneous heat and mass transfer process, particularly on thin film flows. In an absorption process, molecules in the vapor flow are transferred into the liquid flow. To maintain an exothermal absorption process, the heat released in this process must be rejected from the system. Most of these studies were focused on the absorption processes in binary mixtures, particularly in the lithium bromine/water and the ammonia–water mixtures. In absorption systems with the lithium bromine/water mixture, water is the refrigerant, and lithium bromine serves as the absorbent. The absorbent lithium bromine is nonvolatile. Refrigerant, the vapor, does not contain lithium bromine and the vapor in these systems is a single component water steam. Thus, the mass transfer aspect of the problem only exists in the liquid phase. In absorption systems with the ammonia–water mixture, ammonia is the refrigerant, and water serves as the absorbent. The absorbent water is volatile, and thus the vapor in the system contains water as well. In these systems the vapor flow is an ammonia–water mixture. Therefore, the overall mass transfer in the system also depends on the mass transfer within the vapor phase. Because of this, the absorption process in the ammonia–water system is more complicated than that in the lithium bromine/water system.

Among the published literature on the heat and mass transfer studies in the absorption process, most of the effort is devoted to the absorption process in the lithium bromine/water system, where the mass transfer primarily only occur in the liquid flow. There are only a few papers focusing on the mass transfer aspect of an ammonia/water absorption system. This may be due to the fact that the dominant solution pair in commercial absorption machines is the lithium bromine/water solution. A theoretical model for such a system involving absorption of vapor into liquid films and drops was established by Nakoryakov and Grigoreva

* Corresponding author. Creare Inc, Etna Road, PO Box 71, Hanover, NH 03755, USA. Tel.: +603-643-3800; fax: +603-643-4657.

E-mail address: wbc@creare.com (W. Chen)

0017-9310/00/$ - see front matter
PII: S0017-9310(99)00147-7

[1] which includes the influence of temperature variation in the direction of flow. Their paper suggests the existence of subcooling in the bulk liquid region. While Nakoryakov and Grigoreva assumed a uniform velocity profile across the film, Grossman [2] used the general diffusion and energy equations simultaneously to analyze the heat and mass transfer phenomena in the process of the absorption of vapor into the laminar liquid film. By using the method of separation of variables, the author obtained an analytical expression for the film concentration in the form of an infinite series of eigenfunctions. Conlisk [3] used Laplace transforms to obtain a temperature distribution in a very thin film. Numerical techniques were employed to obtain quantitative results. Mass flux, temperature distribution and film thickness were obtained, and compared with experimental results. It was shown in this paper that mass transfer took place in a thin layer of fluid near the liquid–vapor interface, which indicates that mass transfer is dominated by the resistance within the liquid film flow.

Most of these analytical methods cannot be applied to the absorption process for ammonia–water vapor, which is a binary mixture and for which mass transfer resistance also exists in the vapor phase. Among the few papers on ammonia–water absorption processes, the work by Conlisk and Mao [4] is particularly worth mentioning. To our best knowledge, this is the first analytical work on the ammonia–water absorption process. They extend Conlisk's study [3] on the absorption process in a lithium bromine solution to that in an ammonia–water solution. They developed a mathematical model for the absorption process of ammonia–water into the liquid film on a horizontal tube. The boundary condition for mass fraction in the film at the interface is modified to account for the effect of the vapor. The resulting partial differential equations were then solved by using a Fourier cosine transform. In their paper, it was found that the diffusion effect in the vapor had negligible effect on the absorption in the liquid film.

If the diffusion effect in the vapor indeed has negligible effect on the absorption in the liquid film, one can formulate and analyze the problem of absorption of ammonia–water vapor into a liquid film falling over a flat wall in a similar way as Conlisk [3] did for absorption of water vapor into lithium bromine/water thin film. However, Conlisk only found implicit solutions for cases with $\varepsilon\ Re_l\ Pr_l \ll 1$ and $\varepsilon\ Re_l\ Pr_l \sim 1$, and $\varepsilon\ Re_l\ Sc_l \gg 1$, where ε is the ratio of film thickness h^* to film characteristic length L, $\varepsilon = h_0^*/L$, Re_l is the liquid film Reynolds number, Pr_l is the Prandtl number of liquid solution, and Sc_l is the Schmidt number of liquid solution. Complicated numerical techniques were needed to solve the implicit integral equation to obtain the explicit temperature and concentration profiles.

In practical ammonia–water absorption systems, the value of $\varepsilon\ Re_l\ Pr_l$ can range from 0.25 to 50, and the value of $\varepsilon\ Re_l\ Sc_l$ from 5 to 1000. Thus, one of the efforts of this paper is to find solutions for general cases in ammonia–water absorption systems. Furthermore, this paper reports results on a study of the effect of the inlet subcooling on the heat and mass transfer coefficients in an absorption process.

2. Model and governing equations

2.1. Physical problem

This paper will focus on the problem of absorption of ammonia–water vapor into a liquid film falling over a flat wall. The geometry of the problem is shown in Fig. 1. A film of low concentration hot liquid solution flows from the top of an absorber, and a higher concentration cold vapor mixture flows up from the bottom of the absorber. This vapor is absorbed into the low concentration liquid film. This is an exothermal

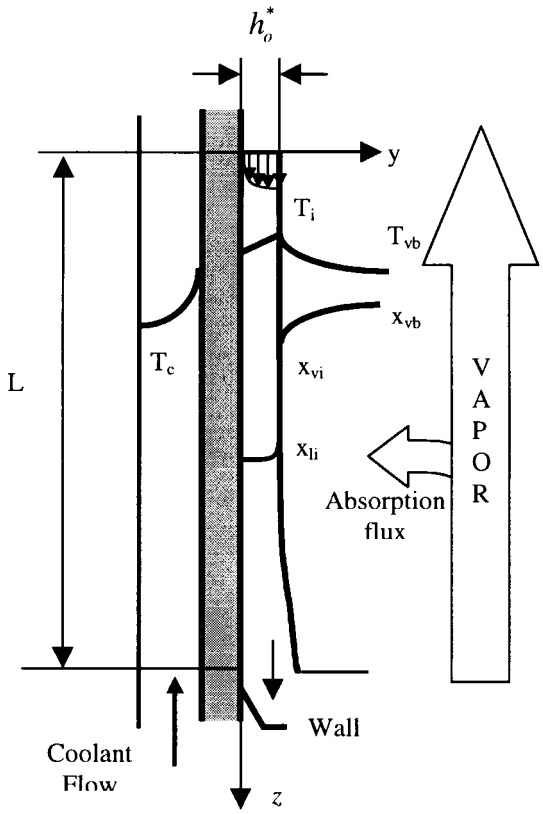

Fig. 1. Typical temperature and concentration profiles during a countercurrent absorption process.

process where latent heat is released at the interface between the film and the vapor. The saturation concentration of ammonia in an ammonia–water solution increases with decrease in the temperature of the solution. Therefore, it is necessary to continuously cool the liquid film. Otherwise, the latent heat released during the absorption process would warm up the film to a point where the film will no longer be able to absorb more ammonia from the vapor. Thus, in order to continue the absorption of ammonia vapor, the liquid film must be cooled by the coolant on the other side of the wall. Fig. 1 also shows the typical temperature and concentration profiles in the liquid and vapor across the flow direction. As mentioned before, in an absorption process, absorption heat is released at the interface, and the liquid film is cooled down at the wall. Thus, the temperature at the interface is the highest for liquid flow along the width of the film. Because ammonia is absorbed into the liquid through the interface, the ammonia concentration is highest at the interface.

From a heat and mass transfer point of view, it is desirable to frequently break the thermal and concentration boundaries of the thin film flow, thereby maintaining a thin thermal boundary layer and a thin species boundary layer. This can be accomplished by frequently mixing the liquid flow at a small interval, say at a distance of L. In the following discussion, only the film within a mixing interval is analyzed, not the entire film in the absorber. It is also assumed that at the beginning of each interval, the solution is well mixed, and the temperature and concentration of the liquid are uniform across the film.

To further simplify the problem, the following assumptions are made in this paper.

1. The liquid is Newtonian and has constant physical properties.
2. Momentum effects and shear stress at the free surface are negligible.
3. The film is a laminar film with no wave at the interface.
4. Absorption within any interval is small compared to the mass flow rate in the film.
5. Thermodynamic equilibrium exists between the vapor and liquid at the interface.
6. All absorption heat is released at the interface.
7. Temperature and concentration at the inlet are uniform.
8. There is no Soret effect.

3. Fluid dynamics

In most cases, the absorption rate is very small compared to the liquid film flow rate. Therefore, within each interval, one can assume that the film thickness is constant. This assumption, along with the zero shear stress assumption will enable the complete decoupling of the momentum equations for the liquid flow from that for the vapor flow.

Because of the low absorption rate, the change of the liquid velocity component in the flow direction is negligible in the flow direction. The nondimensional liquid velocity component in the flow direction, $\tilde{w}$, thus can be expressed by the Nusselt expression [4]:

$$\tilde{w}_1 = Re\,Fr(\tilde{y}h - \tilde{y}^2/2) \tag{1}$$

where $Re = U_0^* h_0^*/\nu_1$ is a Reynolds number, $Fr = gh_0^*/U_0^{*2}$ is a Froude number, and $U_0^* = gh_0^{*2}/\nu_1$ is the characteristic velocity. All distances normal to the wall are nondimensionalized by the initial film thickness h_0^* and the axial coordinate by the film length L [3,4].

4. Heat and mass transfer

Conlisk [3] showed that for a thin film flow, the diffusion term in the flow direction and the convection term across the flow direction can be neglected. Thus, the governing equation for the heat and mass transfer can be written as

$$\frac{1}{\varepsilon\, Re_1\, Pr_1}\frac{\partial^2\theta_1}{\partial\eta^2} = \tilde{w}_1(\eta)\frac{\partial\theta_1}{\partial\zeta},$$
$$\frac{1}{\varepsilon\, Re_1\, Sc_1}\frac{\partial^2\omega_1}{\partial\eta^2} = \tilde{w}_1(\eta)\frac{\partial\omega_1}{\partial\zeta} \tag{2}$$

where $\theta = [(T - T_{\mathrm{sat,in}})/h_{\mathrm{fg}}/c_{\mathrm{p,l}}]$ is the nondimensionalized temperature, and $\omega = [(x - x_{\mathrm{l,in}})/(x_{\mathrm{vi,in}} - x_{\mathrm{l,in}})]$ is the nondimensionalized ammonia concentration. The reference concentration difference, $x_{\mathrm{vi,in}} - x_{\mathrm{li,in}}$, is the interface ammonia concentration difference between the saturated vapor and liquid at the entrance. The problem is solved in an adaptive coordinate system (η, ζ) defined by $\eta = \tilde{y}/h$ and $\zeta = \tilde{z}$ [3]. In this new coordination system, the interface is always located at $\eta = 1$.

One should note that the nondimensionalization for temperatures in this paper is different from that in Conlisk's paper [3]. In this paper, the reference temperature is $T_{\mathrm{sat,in}}$, which is the saturated solution temperature corresponding to the inlet liquid concentration, $x_{\mathrm{l,in}}$, not the inlet solution temperature $T_{\mathrm{l,in}}$ used by Conlisk [3]. By definition in this paper, the nondimensional inlet temperature, $\theta_{\mathrm{l,in}}$, is a measure of the subcooling of the inlet solution.

The boundary conditions for the heat transfer equation are straightforward. It is assumed that the heat flux through the wall is uniform and so is the inlet temperature. In addition to this, it is assumed that the sensible heat transfer from vapor flow to the

interface is negligible compared with the latent heat released at the interface associated with the absorption flux. Thus, the heat flux across the interface can be assumed to be proportional to the mass absorbed.

The boundary conditions for the mass transfer equation at the interface, however, are much more complicated. The total ammonia flux across the interface is the sum of the diffusion flux by molecular diffusion and the convection flux accompanied by the condensation flow (net flow). No mass can be accumulated at the interface, and thus the ammonia flux from the vapor to the interface must be identical to the flux from the interface to the liquid. Therefore:

$$-D_l\rho_l\frac{\partial x_l}{\partial y}+m_c''(z)x_{li}=-D_v\rho_v\frac{\partial x_v}{\partial y}+m_c''(z)x_{vi} \quad \text{at } y=h^*(z) \tag{3}$$

where D_l and D_v are the liquid and vapor diffusion coefficients, respectively, and m_c'' is the mass absorption flux. This boundary condition shows that mass transfer in the liquid film is affected by the conditions in the vapor flow.

The interface vapor concentration on the right-hand-side of Eq. (3) can be directly obtained from the interface temperature by the thermodynamic relation. The vapor concentration gradient at the interface, however, is not yet known. In order to examine the order-of-magnitude of the diffusion term on the vapor side, Eq. (3) is nondimensionalized as:

$$-\frac{1}{\varepsilon\, Re_l\, Sc_l}\frac{\partial\omega_l}{\partial\tilde{y}}=-\frac{\rho_v D_v}{\varepsilon\rho_l U_0^* L_v}\frac{\partial\omega_v}{\partial\tilde{y}_v}+\tilde{m}_c'' +O\left(\frac{x_{vi}-x_{li}}{x_{vi,\,in}-x_{l,\,in}}-1\right) \tag{4}$$

where $\tilde{m}_c''=m_c''/\varepsilon\rho_l U$ is the nondimensional mass absorption flux, and L_v is the characteristic flow length of the vapor flow. The concentration difference between the vapor and liquid flows at the interface, $x_{vi}-x_{li}$, varies very little along a short film, say several centimeters long, and thus the last term on the right-hand-side of Eq. (4) can be neglected.

One can further show that the first term on the right-hand-side of Eq. (4) is negligible in a counterflow absorber. In a counterflow absorber, as the gas velocity is gradually increased, a point would eventually be reached at which large waves are formed on the interface, resulting in a chaotic flow pattern with liquid droplets being entrained by the upward gas flow. This phenomenon is referred to as flooding. Any occurrence of flooding would reduce the liquid flow rate substantially, resulting in a malfunctioning absorber. Thus, in order to avoid the occurrence of flooding, the maximal gas velocity should not exceed the threshold of flooding. Because of this limitation on the gas velocity, the diffusion effect on the vapor side is restrained. Chen [5] extended the analysis carried out by Conlisk and Mao [4] to an actual Generator/Absorber Heat Exchanger (GAX) ammonia/water absorption system, and showed that the diffusion effects in the vapor flow contribute less than 5% of ammonia being absorbed into the liquid solution. Thus, the first term on the right-hand-side of Eq. (4) can be neglected in the first-order analysis, and the boundary condition at the interface for the mass transfer equation can be simplified as

$$-\frac{1}{\varepsilon\, Re_l\, Sc_l}\frac{\partial\omega_l}{\partial\tilde{y}}=\tilde{m}_c''(\tilde{z}) \tag{5}$$

The mass transfer boundary conditions at other locations are straightforward. The other boundary conditions are (a) uniform concentration of ammonia at the inlet and (b) the zero ammonia flux through the wall. The boundary conditions for the heat and mass transfer equations can be summarized as

$$\theta_l(\eta,0)=\theta_{l,\,in}\quad \omega_l(\eta,0)=0$$

$$-\frac{1}{\varepsilon\, Re_l\, Pr_l}\frac{\partial}{\partial\eta}\theta_l(0,\zeta)=\tilde{q}_w'' \quad \frac{\partial}{\partial\eta}\omega_l(0,\zeta)=0$$

$$-\frac{1}{\varepsilon\, Re_l\, Pr_l}\frac{\partial}{\partial\eta}\theta_l(1,\zeta)=\tilde{m}_c''(\zeta) \quad -\frac{1}{\varepsilon\, Re_l\, Sc_l}\frac{\partial}{\partial\eta}\omega_l(1,\zeta)=\tilde{m}_c''(\zeta) \tag{6}$$

where $\tilde{q}_w''=(q_w''h^*c_p/\varepsilon\, Re_l\, Pr_l\, kh_{fg})$ is the nondimensional heat flux at the wall. One should note that the absorption flux $\tilde{m}_c''$ on the boundary conditions (6) is still an unknown variable. One additional equation is needed to determine $\tilde{m}_c''$. This equation can be the thermodynamic relation between the temperature and concentration at the equilibrium state. At constant pressure, the saturated liquid and vapor ammonia concentration can be locally approximated as a linear function of temperature. The nondimensional temperature and nondimensional concentration can be related by the following equation:

$$\theta_l=\beta\omega_l \tag{7}$$

where β is a constant coefficient

5. Controlling parameters for the absorption process

The governing equation set (2), along with boundary conditions (6) and (7), shows that for a particular film flow, the mass absorption process is uniquely deter-

mined by the θ_{in}, q''_w, $\varepsilon\ Re_l\ Pr_l$ and $\varepsilon\ Re_l\ Sc_l$. The governing equations and the boundary conditions are all linear. Thus, the effects of the inlet subcooling θ_{in} and the heat flux through the wall $\tilde{q}''_w$ can be directly superimposed. In order to investigate their contributions to the mass absorption rate, one can decompose the original problem into two separated problems. Assume

$$\frac{1}{\varepsilon\ Re_l\ Pr_l}\frac{\partial^2\theta_{l,1}}{\partial\eta^2}=\tilde{w}_1(\eta)\frac{\partial\theta_{l,1}}{\partial\zeta}$$

$$\frac{1}{\varepsilon\ Re_l\ Sc_l}\frac{\partial^2\omega_{l,1}}{\partial\eta^2}=\tilde{w}_1(\eta)\frac{\partial\omega_{l,1}}{\partial\zeta}$$

with

$$\theta_{l,1}(\eta,0)=\theta_{l,in}\quad\omega_{l,1}(\eta,0)=0$$

$$\frac{\partial}{\partial\eta}\theta_{l,1}(0,\zeta)=0\quad\frac{\partial}{\partial\eta}\omega_{l,1}(0,\zeta)=0$$

$$-\frac{1}{\varepsilon\ Re_l\ Pr_l}\frac{\partial}{\partial\eta}\theta_{l,1}(1,\zeta)=\tilde{m}''_{c,1}(\zeta)$$

$$-\frac{1}{\varepsilon\ Re_l\ Sc_l}\frac{\partial}{\partial\eta}\omega_{l,1}(1,\zeta)=\tilde{m}''_{c,1}(\zeta)$$

$$\theta_{l,1}(1,\zeta)=\beta\omega_{l,1}(1,\zeta)\tag{8}$$

and

$$\frac{1}{\varepsilon\ Re_l Pr_l}\frac{\partial^2\theta_{l,2}}{\partial\eta^2}=\tilde{w}_1(\eta)\frac{\partial\theta_{l,2}}{\partial\zeta}$$

$$\frac{1}{\varepsilon\ Re_l\ Sc_l}\frac{\partial^2\omega_{l,2}}{\partial\eta^2}=\tilde{w}_1(\eta)\frac{\partial\omega_{l,2}}{\partial\zeta}$$

with

$$\theta_{l,2}(\eta,0)=0\quad\omega_{l,2}(\eta,0)=0$$

$$-\frac{1}{\varepsilon\ Re_l\ Pr_l}\frac{\partial}{\partial\eta}\theta_{l,2}(0,\zeta)=\tilde{q}''_w\quad\frac{\partial}{\partial\eta}\omega_{l,2}(0,\zeta)=0$$

$$-\frac{1}{\varepsilon\ Re_l\ Pr_l}\frac{\partial}{\partial\eta}\theta_{l,2}(1,\zeta)=\tilde{m}''_{c,2}(\zeta)$$

$$-\frac{1}{\varepsilon\ Re_l\ Sc_l}\frac{\partial}{\partial\eta}\omega_{l,2}(1,\zeta)=\tilde{m}''_{c,2}(\zeta)$$

$$\theta_{l,2}(1,\zeta)=\beta\omega_{l,2}(1,\zeta)\tag{9}$$

where

$$\tilde{m}''_{c,2}(\zeta)=\tilde{m}''_c(\zeta)-\tilde{m}''_{c,1}(\zeta)\tag{10}$$

$\theta^{l,1}$ and $\omega_{l,1}$ in equation set (8) are the temperature and concentration of a film flow with subcooling θ_{in} at the inlet flowing along an adiabatic wall, while $\theta_{l,2}$ and $\omega_{l,2}$ in equation set (9) are the temperature and concentration of a film flow saturated at the inlet flowing along a cooled wall. By superimposing equation sets (8) and (9), one can find that

$$\theta_l(\eta,\zeta)=\theta_{l,1}(\eta,\zeta)+\theta_{l,2}(\eta,\zeta)\tag{11}$$

$$\omega_1(\eta,\zeta)=\omega_{l,1}(\eta,\zeta)+\omega_{l,2}(\eta,\zeta)\tag{12}$$

These two equations prove that the subcooling effect at the entrance and the cooling effect from the wall may be directly superimposed. They independently affect the absorption process. The total mass absorbed is the sum of the mass absorbed owing to the subcooling at the inlet, $\tilde{m}''_{c,1}$, and the mass absorbed owing to the cooling by a coolant, $\tilde{m}''_{c,2}$.

6. Numerical results

There is no general explicit analytical solution for equation set (2) with boundary condition set (6) and (7). Conlisk [3] obtained analytical solutions in the Laplace transform space for the case with $\varepsilon\ Re_l\ Pr_l \ll 1$ or ~ 1 and $\varepsilon\ Re_l\ Sc_l \gg 1$. Numerical techniques were then used to obtain the inversion of the solutions in a transform domain. The solution obtained by Conlisk is somewhat restrictive in its range of applicability. The range of values of $\varepsilon\ Re_l\ Pr_l$ and $\varepsilon\ Re_l\ Sc_l$ depends on the mixing distance L in addition to the film thickness and the physical properties of the liquid solution. In practical absorption systems, the value of L can range from half a centimeter to several meters. The corresponding value of $\varepsilon\ Re_l\ Pr_l$ ranges from 0.25 to 50, and the value of $\varepsilon\ Re_l\ Sc_l$ from 5 to 1000. Since there is no explicit analytical solution in this range, the differential equations were solved numerically. The primary procedures to solve equation set (2) begin with assuming a value of absorption flux $\tilde{m}''_c$ at each interface location. With this boundary condition, along with a corresponding boundary condition in Eq. (6), the heat and mass transfer equation were then solved separately by a straightforward numerical procedure. The interface temperature and concentration at each location were obtained. If the interface temperature and concentration satisfied the equilibrium condition described by Eq. (7), the assumption on the interface absorption flux $\tilde{m}''_c$ was correct, and the calculation stopped. Otherwise, the value of absorption flux $\tilde{m}''_c$ at each interface location was modified accordingly, and the heat and mass transfer equation were solved. The

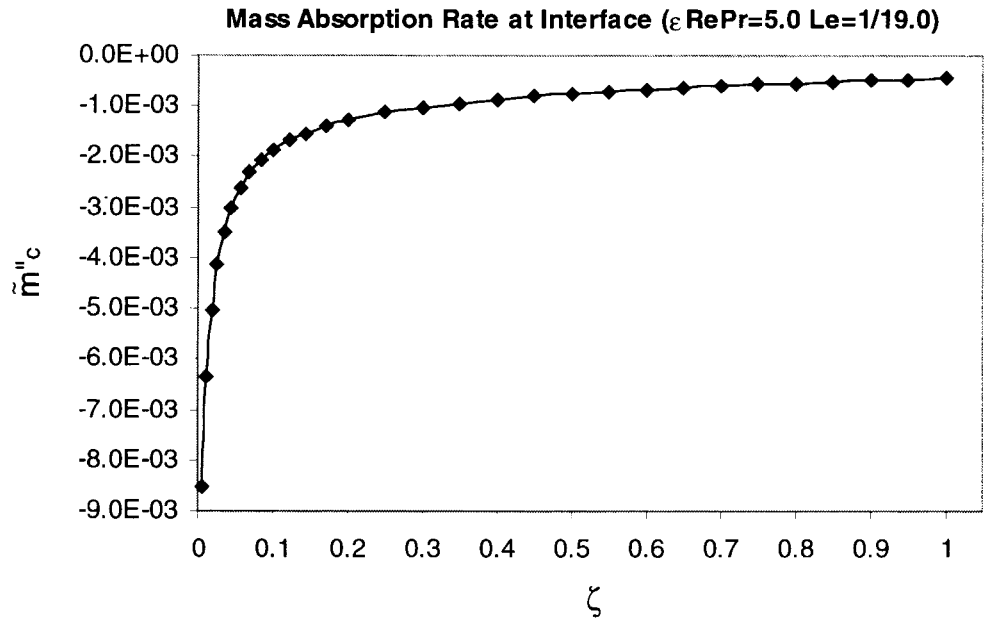

Fig. 2. Nondimensional mass absorption flux at the interface for subcooled inlet solution.

iterative calculation continued until Eq. (7) was satisfied.

Figs. 2 and 3 illustrate the important difference in the mass absorption rate between a case with inlet subcooling and an adiabatic back wall, and a case without inlet subcooling and a cooled back wall. Numerical computation for these cases was done for ε Re_l $Pr_l = 5.0$ and Le = 1/19.0. The results for other parameters, such as temperature, concentration and subcooling were shown in Chen's dissertation [5].

In the case with inlet subcooling, the concentration of ammonia within the film at the entrance is less than the saturated concentration corresponding to the inlet temperature. As soon as the flow enters the section,

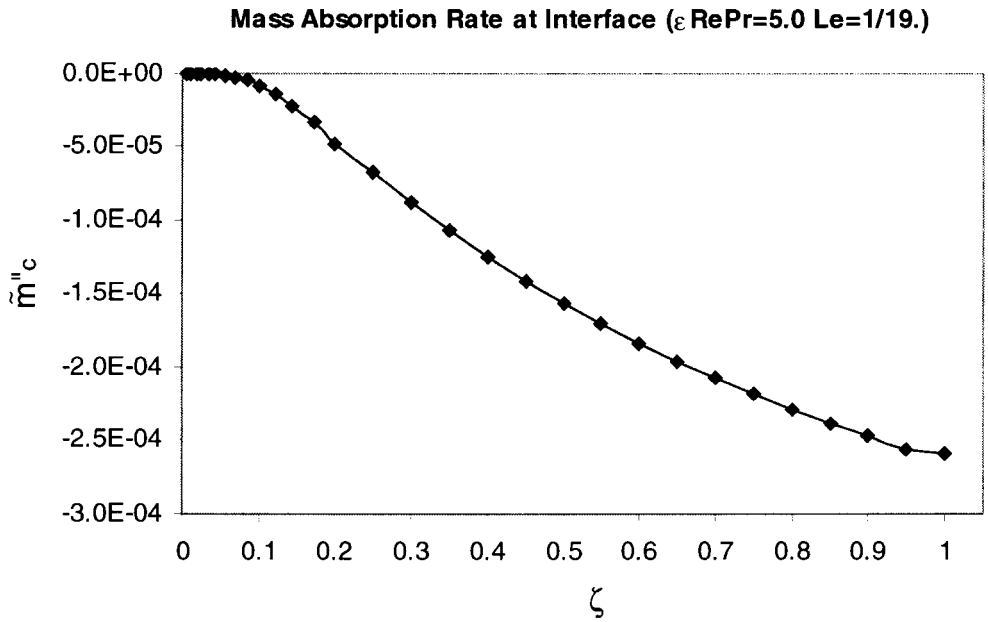

Fig. 3. Nondimensional mass absorption flux at the interface for saturated inlet solution.

the interface becomes saturated with ammonia. This leads to an infinitely large concentration gradient at the interface and an infinitely large absorption flux. This is similar to the development of a boundary layer at the leading edge of a flat plate. Soon a boundary layer develops inside the liquid film. In addition, due to the exothermic heat released at the interface, the film warms up, resulting in a decrease in the interface saturation concentration of ammonia. Both these factors leads to a reduction in the concentration gradient at the interface and hence, a reduced absorption mass flux.

Unlike the previous case with a subcooled inlet solution along an adiabatic wall, for the saturated inlet solution along a cooled wall, the magnitude of the absorption flux increases along the flow direction, as shown in Fig. 3. Since the inlet solution at the entrance is saturated, the interface concentration of ammonia is the same as that in the film. Therefore, at $\zeta=0$ the concentration gradient within the film is zero everywhere and hence, the absorption mass flux is also zero. When the solution flows down the cooled wall, heat is rejected from the solution to the wall and the temperature within the film decreases in the flow direction. This decrease in the interface temperature causes an increase in the interface concentration according to the thermodynamic relationship at the equilibrium state, initiating a concentration gradient at the interface and the absorption process begins. As the thermal boundary layer at the wall grows along the wall, the temperature within the film decreases further, resulting in an increase in the interface concentration gradient along the flow direction and an increase in the absorption flux.

Comparing Fig. 2 with Fig. 3, one can find that the magnitude of the absorption flux in the first case is much larger than the second one. It is generally true that the absorption rate is primarily determined by the degree of subcooling at the inlet for a short mixing distance. But the absorption rate decreases along the flow direction in the first case while it increases in the second case. Thus, if the mixing distance is kept increasing, the mass absorption rate in the second case will eventually dominate the total absorption rate.

As mentioned before, the absorption process in a thin film flow is uniquely determined by the nondimensional parameters $\varepsilon\ Re_l\ Pr_l$, $\varepsilon\ Re_l\ Sc_l$, θ_{in} and $\tilde{q}''_w$. It has also been shown that the nondimensional temperature and concentration are linear functions of θ_{in} and $\tilde{q}''_w$. Thus, one only needs to investigate the effects of $\varepsilon\ Re_l\ Pr_l$ and $\varepsilon\ Re_l\ Sc_l$ to understand the absorption process.

The values of $\varepsilon\ Re_l\ Pr_l$ and $\varepsilon\ Re_l\ Sc_l$ depend upon the mixing distance of the flow L in addition to other parameters. Thus, if the numerical solution for a film flow within mixing distance L is obtained, the solution for $\tilde{z}=0$ to λL $(0<\lambda<1)$ can be used to obtain the results for a film with $\varepsilon\ Re_l\ Pr_l/\lambda$ and $\varepsilon\ Re_l\ Sc_l/\lambda$. Therefore, one only needs to perform a few computations for flows with different ratios of $\varepsilon\ Re_l\ Pr_l$ to $\varepsilon\ Re_l\ Sc_l$, or in other words, for flows with a different Lewis number Le, to reveal the effects of $\varepsilon\ Re_l\ Pr_l$ and $\varepsilon\ Re_l\ Sc_l$. Numerical calculations were carried out for different values of $\varepsilon\ Re_l\ Pr_l$ and $\varepsilon\ Re_l\ Sc_l$, and the results were used to develop the following empirical correlations for mass absorption rate, wall temperature and interface temperature:

$$\bar{\tilde{m}}''_c = \bar{\tilde{m}}''_{c,1} + \bar{\tilde{m}}''_{c,2} = \theta_{l,in}\bar{F}_1(\varepsilon\ Re_l\ Pr_l, Le_l) + \tilde{q}''_w\bar{F}_2(\varepsilon\ Re_l\ Pr_l, Le_l) \tag{13}$$

$$\bar{\theta}_w = \bar{\theta}_{w,1} + \bar{\theta}_{w,2} = \theta_{l,in}\bar{G}_1(\varepsilon\ Re_l\ Pr_l, Le_l) + \tilde{q}''_w\bar{G}_2(\varepsilon\ Re_l\ Pr_l, Le_l) \tag{14}$$

$$\bar{\theta}_{l,i} = \bar{\theta}_{li,1} + \bar{\theta}_{li,2} = \theta_{l,in}\bar{H}_1(\varepsilon\ Re_l\ Pr_l, Le_l) + \tilde{q}''_w\bar{H}_2(\varepsilon\ Re_l\ Pr_l, Le_l) \tag{15}$$

The expressions for $\bar{F}_1$, $\bar{F}_2$, $\bar{G}_1$, $\bar{G}_2$, $\bar{H}_1$, and $\bar{H}_2$ are given in the Appendix.

7. Heat and mass transfer coefficients

The conventional definition of the heat transfer coefficient, h_q, for a thin film is the ratio of the heat flux through the wall, q''_w, to the temperature difference between the wall and the interface, T_w-T_{int}, that is $h_q=q''_w/(T_w-T_{int})$. Following this definition, the average heat transfer coefficient in a short segment may be written as:

$$\bar{h}_q = \frac{q''_w}{(\bar{\theta}_w-\bar{\theta}_{li})\Delta T} = \frac{\varepsilon\ Re_l\ Pr_l\ k_l\bar{\tilde{q}}''_w}{h_0^*(\bar{\theta}_w-\bar{\theta}_{li})} \tag{16}$$

As mentioned before, the nondimensional wall temperature and interface temperature are functions of inlet subcooling and heat flux through the wall. By substituting Eqs. (14) and (15) into (16), Eq. (16) can be rewritten as

$$\bar{h}_q = \frac{k_l}{h_0^*}\varepsilon\ Re_l\ Pr_l\left(\frac{\theta_{l,in}}{\bar{\tilde{q}}''_w}(\bar{G}_1-\bar{H}_1)+(\bar{G}_2-\bar{H}_2)\right)^{-1} \tag{17}$$

Eq. (17) shows that the heat transfer coefficient is a

function of $\theta_{\mathrm{l,\,in}}/\bar{\tilde{q}}''_{\mathrm{w}}$, the ratio of subcooling to the nondimensional heat flux through the wall, besides being a function of the film thickness, the thermal conductivity and other flow parameters. Only when the subcooling of the inlet solution is zero, will the heat transfer coefficient become independent of the heat flux through the wall.

Fig. 4 shows effects of the nondimensional parameter $\varepsilon\ Re_{\mathrm{l}}\ Pr_{\mathrm{l}}$ and the nondimensional inlet subcooling on the nondimensional heat transfer coefficients $h_q/(k_{\mathrm{l}}/h_0^*)$. When $\varepsilon\ Re_{\mathrm{l}}\ Pr_{\mathrm{l}}$ increases, the convection effect becomes more significant. Thus, the nondimensional heat transfer coefficient increases with $\varepsilon\ Re_{\mathrm{l}}\ Pr_{\mathrm{l}}$. Fig. 4 also shows that the heat transfer coefficient is significantly affected by the subcooling of the inlet solution. Any increase in the degree of subcooling at the inlet will raise the temperature difference between the interface and the wall. As a result, the value of the heat transfer coefficient will decrease. Fig. 4 also indicates that when the inlet solution is not severely subcooled, the heat transfer coefficient of a binary mixture in an absorption process is larger than that of a single component fluid in a condensation process, which may be estimated by Nusselt's prediction.

Similar to the definition of a heat transfer coefficient, the average mass transfer coefficient of a film flow is defined as

$$\bar{h}_{\mathrm{m,\,l}} = \frac{\bar{m}''_{\mathrm{c}}}{c_{\mathrm{l,\,i}} - c_{\mathrm{l,\,bulk}}} = \frac{\bar{m}''_{\mathrm{c}}}{c_{\mathrm{l,\,i}} - (c_{\mathrm{l,\,in}} + \bar{m}''_{\mathrm{c}} L/2\Gamma)} = \frac{D}{h_0^*}\varepsilon \qquad (18)$$

$$Re_{\mathrm{l}}\, Sc_{\mathrm{l}} \frac{\bar{\tilde{m}}''_{\mathrm{c}}}{\bar{\theta}_{\mathrm{int}}(x_{\mathrm{vi,\,in}} - x_{\mathrm{l,\,in}})/\beta - 3\bar{\tilde{m}}''_{\mathrm{c}}/2}$$

Fig. 5 shows the effects of the nondimensional parameters $\varepsilon\ Re_{\mathrm{l}}\ \mathrm{Pr_l}$ and the nondimensional inlet subcooling on the average nondimensional mass transfer coefficient $h_{\mathrm{m}}/(D_{\mathrm{l}}/h_0^*)$. The convection effect becomes more significant as $\varepsilon\ Re_{\mathrm{l}}\ Pr_{\mathrm{l}}$ increases. Thus, the concentration boundary layer at the interface becomes thinner, and the nondimensional mass transfer coefficient increases. For a subcooled inlet solution flowing along an adiabatic wall, the interface concentration approaches to a constant value asymptotically. For a saturated inlet solution following along a cooled wall, however, the mass flux across the interface approaches a constant value asymptotically. Thus, the mass transfer coefficient for the first case is lower than the second case. Any general case can be considered as a linear

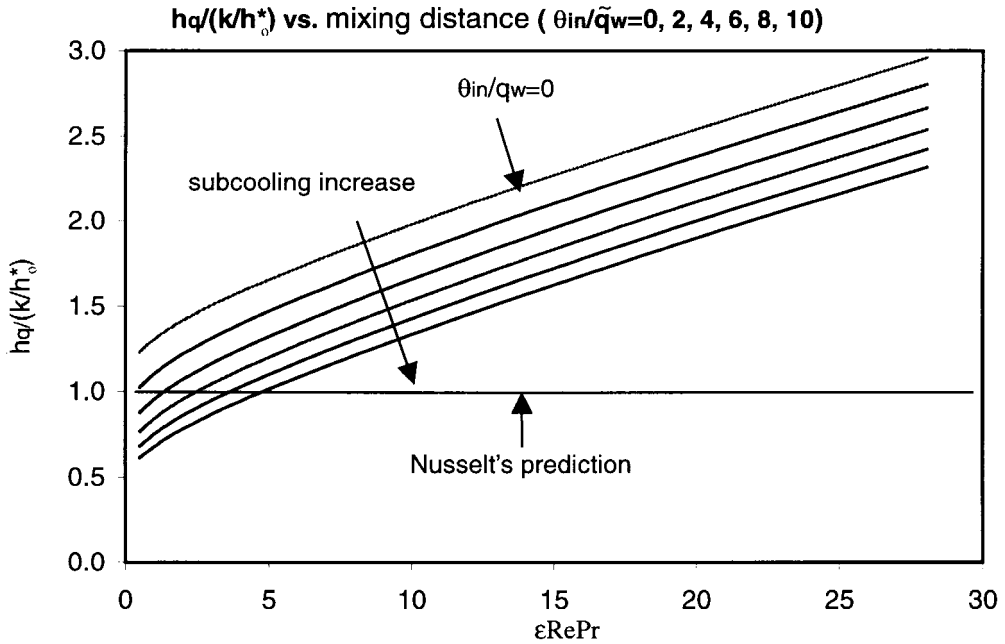

Fig. 4. Effect of nondimensional parameter $\varepsilon\ Re_{\mathrm{l}}\ Pr_{\mathrm{l}}$ on the average nondimensional heat transfer coefficient of the film with $Sc/Pr = 20$.

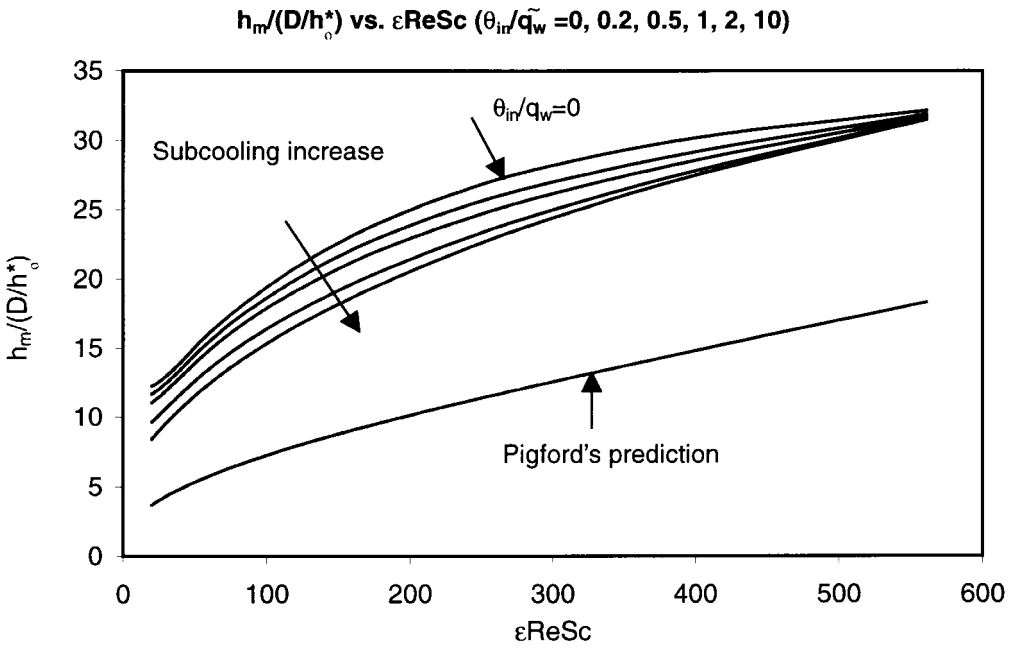

Fig. 5. Effect of nondimensional parameters $\varepsilon\ Re_l\ Pr_l$ on the average nondimensional mass transfer coefficient of the film with $Sc/Pr = 20$.

combination of these two cases, and hence, any subcooling at the inlet results in a decrease in the mass transfer coefficient.

For the purpose of comparison, the result for an isothermal absorption process is plotted in Fig. 5. This analytical result was obtained by Pigford [6] for the absorption rate by a liquid film with a parabolic velocity distribution. In his problem, the liquid feed has a uniform concentration $c_{l,in}$ and the surface of the falling film is maintained at a constant concentration $c_{li,in}$. Using the method of separation variables, he obtained an analytical solution in a series for the average outlet liquid concentration over a column length of L, $c_{l,out,ave}$, which can be written in terms of nondimensional variables defined in this paper as

$$\frac{c_{l,\,out,\,ave} - c_{li,\,in}}{c_{l,\,in} - c_{li,\,in}} = 0.7857e^{-10.242/\varepsilon ReSc} + 0.1001e^{-78.42/\varepsilon ReSc} + 0.0360e^{-211.2/\varepsilon ReSc} + 0.0181e^{-405.4/\varepsilon ReSc} + \cdots \quad (19)$$

The corresponding mass transfer coefficient based on arithmetic average concentration difference thus can be expressed as:

$$h_m = \frac{2}{3}\frac{D}{h^*}\varepsilon\, Re\, Sc \frac{1 - \dfrac{c_{l,\,out,\,ave} - c_{li,\,in}}{c_{l,\,in} - c_{li,\,in}}}{1 + \dfrac{c_{l,\,out,\,ave} - c_{li,\,in}}{c_{l,\,in} - c_{li,\,in}}} \quad (20)$$

Fig. 5 shows that the mass transfer coefficient based on the present study has a higher value than Pigford's prediction. The difference between the two is mainly because the absorption process considered in this paper is a simultaneous heat and mass transfer process, while the prediction on Pigford's work is for an isothermal process. In a simultaneous heat and mass transfer process, material is transferred to the liquid flow not only by molecular diffusion, but also by flow convection, such as a flow condensation. Thus, the mass transfer coefficient in an exothermal process is higher than an isothermal process.

Knowing the heat and mass transfer coefficients on the liquid side, as well as the knowledge on the heat and mass transfer on the vapor side, one can use the Colburn–Drew equation to design and analyze a heat and mass exchanger. A general design procedure has been described in detail by Price and Bell [7] and Kang [8], etc. Chen [5] also illustrated the application of the heat and mass transfer models developed in this paper to the design of a compact counterflow absorber for an ammonia–water absorption heat pump system.

8. Summary

This paper demonstrates that the overall absorption process can be decomposed to two basic processes: absorption owing to the subcooling and absorption owing to the cooling effect of the wall. These two pro-

cesses can be directly superimposed. In the case with a subcooled inlet solution, the mass absorption rate decreases rapidly along the liquid flow direction. In the other case, the mass absorption rate increases asymptotically along the liquid flow direction. For short mixing distances, the absorption rate is controlled by the subcooling at the inlet.

Empirical correlations for the absorption rate, the wall temperature and the interface temperature were achieved for $\varepsilon\ Re\ Pr$ ranging from 0.5 to 50, and $\varepsilon\ Re\ Sc$ from 5 to 3000. By using these empirical correlations, the heat and mass transfer correlations for thin film flows in the absorption process were obtained. These correlations include the entrance and subcooling effects. The correlations indicate that the average heat and mass transfer coefficients in the absorption process are affected by the subcooling of the solution, as well as the film thickness and the fluid properties. If the inlet solution is saturated, the heat transfer coefficient for binary mixtures is larger than that for single component fluid, and the mass transfer coefficient for exothermal processes is larger than that for isothermal processes.

Appendix. Empirical correlations for nondimensional mass absorption flux, interfacial temperature and wall temperature

$$\bar{\tilde{m}}''_{c} = \bar{\tilde{m}}''_{c,1} + \bar{\tilde{m}}''_{c,2} = \theta_{l,in}\bar{F}_1(\varepsilon\, Re_l\, Pr_l, Le_l) + \tilde{q}'_w\bar{F}_2(\varepsilon\, Re_l\, Pr_l, Le_l)$$

where

$$\bar{F}_i(\varepsilon\, Re_l\, Pr_l, Le_l) = (1 + f_{i,7}/(\varepsilon\, Re_l\, Pr_l)^{1/2} + f_{i,8}\, Le_l + f_{i,9}\, Le_l^2)\Phi_i$$

$$\Phi_i = \begin{cases} f_{i,1} + f_{i,2}(\varepsilon\, Re_l\, Pr_l) + f_{i,3}(\varepsilon\, Re_l\, Pr_l)^2 + f_{i,4}(\varepsilon\, Re_l\, Pr_l)^3 & \text{if } \varepsilon\, Re_l\, Pr_l < 1 \\ f_{i,5}(\varepsilon\, Re_l\, Pr_l)^{f_{i,6}} & \varepsilon\, Re_l\, Pr_l > 10 \end{cases} \tag{21}$$

$f_{1,1} = 0.047178 \quad f_{1,2} = -0.00183 \quad f_{1,3} = -0.0002$

$f_{1,4} = 2.150\text{E}-05 \quad f_{1,5} = 0.078251 \quad f_{1,6} = -0.4265$

$f_{1,7} = 1.746273 \quad f_{1,8} = 52.49933 \quad f_{1,9} = -284.355$

$f_{2,1} = 0.099576 \quad f_{2,2} = -0.01911 \quad f_{2,3} = 0.001781$

$f_{2,4} = -6.7\text{E}-05 \quad f_{2,5} = 0.794371$

$f_{2,6} = -1.55759 \quad f_{2,7} = 1.830013 \quad f_{2,8} = 60.36143$

$f_{2,9} = -287.859$

$$\bar{\theta}_w = \bar{\theta}_{w,1} + \bar{\theta}_{w,2} = \theta_{l,in}\bar{G}_1(\varepsilon\, Re_l\, Pr_l, Le_l) + \tilde{q}''_w\bar{G}_2(\varepsilon\, Re_l\, Pr_l, Le_l) \tag{22}$$

where

$$\bar{G}_i(\varepsilon\, Re_l\, Pr_l, Le_l) = (1 + g_{i,6}/(\varepsilon\, Re_l\, Pr_l)^{1/2} + g_{i,7}\, Le_l + g_{i,8}\, Le_l^2)\Gamma_i$$

$$\Gamma_i = g_{i,1} + g_{i,2}(\varepsilon\, Re_l\, Pr_l)^{g_{i,3}} + g_{i,4}(\varepsilon\, Re_l\, Pr_l)^{g_{i,5}}$$

$g_{1,1} = 0.32344 \quad g_{1,2} = 0.9314 \quad g_{1,3} = -0.01765$

$g_{1,4} = 0.17937 \quad g_{1,5} = -2.41768 \quad g_{1,6} = -0.4770$

$g_{1,7} = -2.84203 \quad g_{1,8} = 13.81213$

$g_{2,1} = 0.90498 \quad g_{2,2} = 1.78219 \quad g_{2,3} = 0.523494$

$g_{2,4} = 0.84504 \quad g_{2,5} = -1.58903 \quad g_{2,6} = -0.49938$

$g_{2,7} = -1.41974 \quad g_{2,8} = 6.593848$

$$\bar{\theta}_{l,i} = \bar{\theta}_{li,1} + \bar{\theta}_{li,2} = \theta_{l,in}\bar{H}_1(\varepsilon\, Re_l\, Pr_l, Le_l) + \tilde{q}''_w\bar{H}_2(\varepsilon\, Re_l\, Pr_l, Le_l) \tag{23}$$

where

$$\bar{H}_i(\varepsilon\, Re_l\, Pr_l, Le_l) = \varepsilon\, Re_l Pr(1 + h_{i,9}\, Le_l + h_{i,10}\, Le_l^2)H_i$$

$$H_i = \begin{cases} h_{i,1} + h_{i,2}(\varepsilon\, Re_l\, Pr_l)^{h_{i,3}} + h_{i,4}(\varepsilon\, Re_l\, Pr_l)^{h_{i,5}} & \text{if } \varepsilon\, Re_l\, Pr_l < 10 \\ h_{i,6} + h_{i,7}(\varepsilon\, Re_l\, Pr_l)^{h_{i,8}} & \varepsilon\, Re_l\, Pr_l > 10 \end{cases}$$

$h_{1,1} = 1.43716 \quad h_{1,2} = 0.91229 \quad h_{1,3} = -0.69873$

$h_{1,4} = -1.623774 \quad h_{1,5} = -0.02674 \quad h_{1,6} = 0.0011$

$h_{1,7} = 0.84709 \quad h_{1,8} = -0.96553 \quad h_{1,9} = -7.22182$

$h_{1,10} = 34.28829$

$h_{2,1} = 1.32559 \quad h_{2,2} = 3.00602 \quad h_{2,3} = -0.51915$

$h_{2,4} = -3.241247 \quad h_{2,5} = -0.17349 \quad h_{2,6} = 0.00011$

$h_{2,7} = 4.85143 \quad h_{2,8} = -1.8935 \quad h_{2,9} = -6.48403$

$h_{2,10} = 29.29442$

In the curve fitting, the target is to find the parameters for a particular equation to the minimum sum of the relative errors at each point, which is

$$\sum_{i=1}^{n}\left(\frac{\text{actual value} - \text{predicted value from correlation}}{\text{actual value}}\right)^2$$

The relative errors for each point are shown in the Appendix. The maximum relative error of these correlations is less than 8%. The average relative errors for these correlations are less than 4%.

References

[1] V.E. Nakoryakov, N.I. Grigoreva, Combined heat and mass transfer during absorption in drops and films, Journal of Engineering Physics 32 (1977) 243–247.

[2] G. Grossman, Simultaneous heat and mass transfer in film absorption under laminar flow, International Journal of Heat and Mass Transfer 26 (1983) 357–371.

[3] A.T. Conlisk, Falling film absorption on a cylindrical tube, AIChE Journal 38 (1992) 1716–1726.

[4] A.T. Conlisk, J. Mao, Nonisothermal absorption on a horizontal cylindrical tube—1. The film flow, Chemical Engineering Science 51 (1996) 1275–1285.

[5] W. Chen, Investigation of heat and mass transfer characteristics in an absorber with perforated plates. Ph.D. dissertation, The Ohio State University, Columbus, OH, 1998.

[6] R.L. Pigford, Counter diffusion in a wetted wall column. Ph.D. dissertation, University of Illinois, Urbana, IL, 1941.

[7] B.C. Price, K.J. Bell, Design of binary vapor condensers using the Colburn–Drew equations, AIChE Symposium 70 (1973) 163–171.

[8] Y.T. Kang, W. Chen, R.N. Christensen, A generalized design model by combined heat and mass transfer analysis in NH_3–H_2O absorption heat pump systems, ASHRAE Transaction 102 (1996) 963–972.